19th International Conference on
Adaptive Structures and Technologies
October 6-9, 2008
Ascona, Switzerland

Design, Analysis and Testing of a Smart Fin

Adi Nir[1,2]*and Haim Abramovich[2]
[1] Rafael- Advanced Defense Systems, Israel
[2]Technion- Israel Institute of Technology, Israel

ABSTRACT

The paper presents a design concept for a control fin usually used in airborne vehicles such as UAV's, Micro UAV's and missiles. The research presents the design of a smart fin with integral piezoelectric actuators embedded in the airfoil skin. Electric field applied to the actuators would twist the airfoil leading to a change of the angle of attack. The study presents, analyze and demonstrates various lamination and actuation methods including a parametric performance investigation by finite elements models and closed form analytical model. The design and the theoretical results are verified by a manufactured smart wing demonstrator subjected to series of static and dynamic lab tests.

Keywords: Smart Fin, Embedded Piezoelectric actuators, Twist, Static and Dynamic Tests.

1. INTRODUCTION

The conventional design approach of airborne vehicles such as missiles, UAVs and Micro UAVs include movable control surfaces attached by hinges and actuated by electro-mechanical , pneumatic or hydraulic actuators. As the requirements for airborne vehicles efficiency becomes higher, the need for more efficient control methods is required. In recent years the study of smart materials such as piezoceramic and shape memory alloys have achieved high performance products motivated mainly by the requirements of aerospace industry. By using smart materials to change the shape of airborne vehicle lift surface one can achieve a light weight control surface with minimum drag and maximum aerodynamic efficiency, smart airfoils containing no separately moving parts. In the last decade many studies had been conducted on the application of morphing structures in aerospace industry by academic and research institutes.

In the present study, a design concept for a smart control wing is suggested. The design includes airfoil skin made of passive composite materials combined with active layers of piezoceramic material, and by applying an electrical field on the piezoceramic layers the airfoil is twisted and changes its aerodynamic coefficients.

One of the challenges is to find the optimal design configuration that would achieve high actuation twist angles from one hand and be rigid enough to withstand aerodynamics loads with minimum deflection on the other hand.

A piezoceramic actuator commonly known as Macro Fiber Composite (MFC) was used. This actuator was developed by NASA Langley research center in the year 2000, and the actuator is manufactured today by Smart-Materials Corporation [4] by NASA's license[6]. The actuator is built

from piezoceramic rectangular fibers aligned and spaced equally. On the top and bottom of the fibers integrated electrode pattern on polyamide film are attached. These actuators has relatively low production costs due to the manufacturing methods, high performance strains of up to 1500 μstrain and have a flexible structure suitable for attachment on curved surfaces.

2. DESIGN CONCEPT

The design concept of the smart fin is to change the aerodynamic forces on the fin by creating an active controllable shape morphing of the airfoil's skin. The design presented in the present study creates a twist deformation along the fin span, the twist deformation change the local airfoil AOA but keep the cross section of the airfoil undeformed. An illustration of the smart fin in its deformed shape is presented in Figure 1.

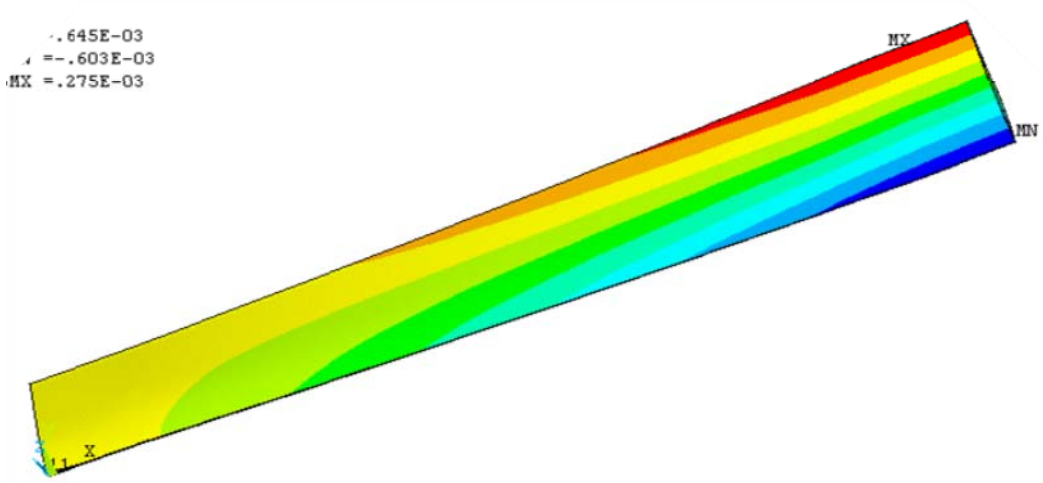

Figure 1: Smart fin ,deformed shape FEM displacements illustration

2-1. Structural Design

Conventional airfoil structural design includes structural spars and ribs or core material covered by a skin. In order to create the twist deformation of the morphing control surface , the skin was made of laminated composite materials, and designed with active piezoelectric layers of MFC with fibers oriented at $+45^{o}/-45^{o}$ which would create the twist deformations . The passive layers of skin are oriented with fibers at $0^{o}/90^{o}$. In the proposed layering configuration the bending strength and stiffness of fin is determined by passive layers and the twist stiffness and strength determined by active layers, meaning that the MFC patches are also part of the structural design. The study deals with parametric performance investigation of the different design parameters like: the layers of the skin, location of the actuators along the span and chord of the airfoil, the active coverage area, applied electrical field polarity and its intensity. The skin of the airfoil is flexible in its active areas and stiffened at the passive areas for best actuation and structural performance (see Figure 2).

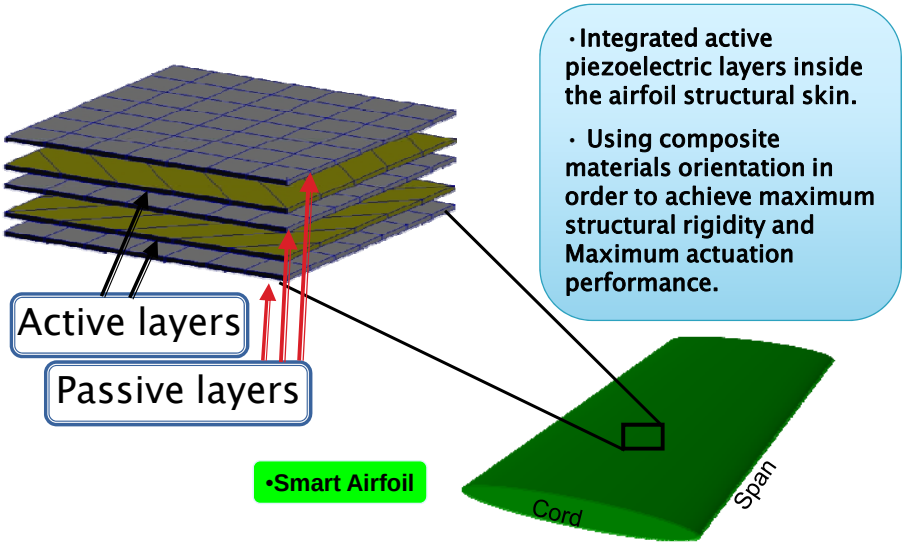

Figure 2: The structural design concept of a smart fin

2-2. Actuation Methods

As already stated before, the design concept suggested herein includes active layers of piezoceramic actuators embedded in the airfoil skin, to create a twist deformation of the fin. Three actuation methods were considered (see Figure 3):

- **Pure Shear Strain**- this method is based on creating pure shear strains (γ_{xy}) in the active skin of the airfoil , the skin laminate being built from non active fibers along the wing span direction and the wing chord direction, while the piezoceramic layers are oriented at +45/-45° . Applying opposite electrical field on the actuators couple will cause elongation for a positive electric field and shortening for a negative one. This will yield deformations along the wing span to eliminate each other and create a pure shear strain. The pure shear strains field in the laminate will create the twisting of the airfoil section. This deformation field resembles the strains developed in closed thin wall shell under a pure twist torque.
- **Skew Bending-** the second actuation system would also cause a twist deformation in the airfoil but the twist displacement is created by curvature radius in the laminate (κ_{xy}) along an inclined axis of 45°. This is achieved by using similar lamination of active layers at +45/-45° angles and by applying electrical field with the same polarity on both active layers. The active layers are separated by non active layers, and each active layer is causing bending effect in the laminate according to the piezoceramic fibers direction.
- **Single Active Layer-** this third actuation system is a combination of the skew bending method and pure shear strain method. Using a single active layer in the skin laminate a combined strain field that would include curvature radius (κ_{xy}) and shear strain (γ_{xy}) is created in the skin laminate.

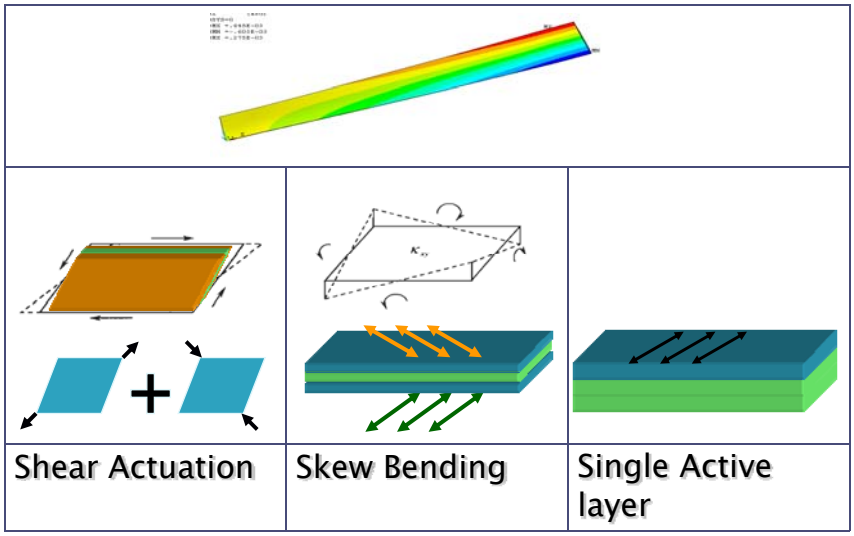

Figure 3: Actuation methods of the smart fin

3. COMPUTATIONAL MODEL

3-1. Shear Actuation Deformation

For the shear actuation method a simple closed form analytic solution was developed, based on the classical lamination theory (CLT) and Kirchoff-Love thin plate theory. The implementation of the theories is described in the following paragraph.

The displacements in a thin plate are a combination of the displacements of its mid-plane (z=0) and the distance from the mid-plane as described in Figure .

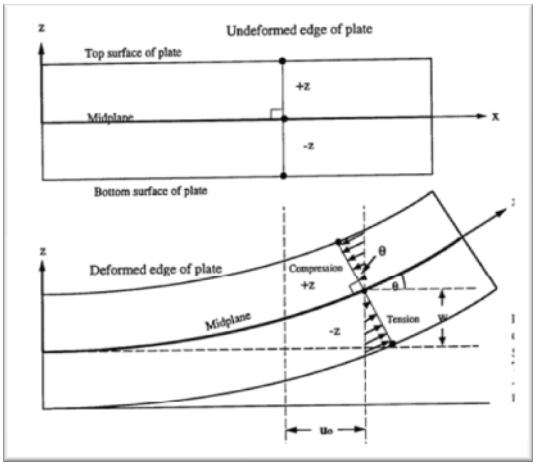

Figure 4: Displacements in thin plates

The mathematical expression is shown in Eq. (1), where ε_{ij}^{0} ,z and K_{ij} are the mid-plane strains, distance from the mid-plane and the plate's curvature radius, respectively.

$$\begin{bmatrix}\varepsilon_x\\ \varepsilon_y\\ \gamma_{xy}\end{bmatrix}=\begin{bmatrix}\varepsilon_x^0\\ \varepsilon_y^0\\ \gamma_{xy}^0\end{bmatrix}+z\cdot\begin{bmatrix}\kappa_x\\ \kappa_y\\ \kappa_{xy}\end{bmatrix} \tag{1}$$

The definition of ε_{ij}^0, z and K_{ij} are given in Eq.(2)

$$\varepsilon^0=\begin{bmatrix}\varepsilon_x^0\\ \varepsilon_y^0\\ \gamma_{xy}^0\end{bmatrix}=\begin{bmatrix}\dfrac{\partial u_0}{\partial x}\\ \dfrac{\partial v_0}{\partial y}\\ \dfrac{\partial u_0}{\partial x}+\dfrac{\partial v_0}{\partial y}\end{bmatrix};\kappa=\begin{bmatrix}\kappa_x\\ \kappa_y\\ \kappa_{xy}\end{bmatrix}=\begin{bmatrix}\dfrac{\partial^2 w_0}{\partial x^2}\\ \dfrac{\partial^2 w_0}{\partial y^2}\\ 2\cdot\dfrac{\partial^2 w_0}{\partial x\partial y}\end{bmatrix} \tag{2}$$

The stresses in the plate are given in Eq. (3), where Q_{ij} are the material stiffness matrix components:

$$\begin{bmatrix}\sigma_x\\ \sigma_x\\ \tau_{xy}\end{bmatrix}=\begin{bmatrix}\bar{Q}_{11}&\bar{Q}_{12}&\bar{Q}_{16}\\ \bar{Q}_{12}&\bar{Q}_{22}&\bar{Q}_{26}\\ \bar{Q}_{16}&\bar{Q}_{26}&\bar{Q}_{66}\end{bmatrix}\begin{bmatrix}\varepsilon_x^0\\ \varepsilon_y^0\\ \gamma_{xy}^0\end{bmatrix}+z\begin{bmatrix}\bar{Q}_{11}&\bar{Q}_{12}&\bar{Q}_{16}\\ \bar{Q}_{12}&\bar{Q}_{22}&\bar{Q}_{26}\\ \bar{Q}_{16}&\bar{Q}_{26}&\bar{Q}_{66}\end{bmatrix}\begin{bmatrix}\kappa_x\\ \kappa_y\\ \kappa_{xy}\end{bmatrix} \tag{3}$$

The load resultant in each material layer is calculated by integration of the stress in the relevant direction, *h* describing the thickness of each material layer.

$$N_x=\int_{-h/2}^{h/2}\sigma_x\partial z \qquad M_x=\int_{-h/2}^{h/2}\sigma_x z\partial z \tag{4}$$

The following assumptions are used for modeling the active twist deformation :

- Cross-sectional shape is maintained during deformation, but out-of-plane displacements are allowed.
- The wall thickness is small compared with the other dimensions so that the problem can be treated as a thin walled, plane stress problem.
- The transverse in-plane normal stresses are negligible (no internal pressure).
- The rate of twist can vary along the length of the beam and it acts as a measure of the torsional warping of the cross-section.

Applying the assumptions on Eq. (4) we get the following reduced form:

$$\begin{Bmatrix}N_x\\ N_{xs}\\ M_x\end{Bmatrix}=\begin{bmatrix}L_{11}&L_{12}&L_{13}\\ L_{12}&L_{22}&L_{23}\\ L_{13}&L_{23}&L_{33}\end{bmatrix}\begin{Bmatrix}\varepsilon_x^0\\ \gamma_{xs}\\ \kappa_x\end{Bmatrix}-\begin{Bmatrix}\overline{N}_x^a\\ \overline{N}_{xs}^a\\ \overline{M}_x^a\end{Bmatrix} \tag{5}$$

In case of shear actuation, it is assumed that the shear strain is applied by the active layers and the external aerodynamic load induces a twisting torque. Because of the linear behavior of this model other effects may be added by superposition. Under those assumptions, we get the one dimensional

form:

$$\begin{Bmatrix} \cancel{N_x} \\ N_{xs} \\ \cancel{M_x} \end{Bmatrix} = \begin{bmatrix} \cancel{L_{11}} & \cancel{L_{12}} & \cancel{L_{13}} \\ \cancel{L_{12}} & L_{22} & \cancel{L_{23}} \\ \cancel{L_{13}} & \cancel{L_{23}} & \cancel{L_{33}} \end{bmatrix} \begin{Bmatrix} \cancel{\varepsilon_x^0} \\ \gamma_{xs} \\ \cancel{\kappa_x} \end{Bmatrix} - \begin{Bmatrix} \cancel{\bar{N}_x^a} \\ N_{xs}^a \\ \cancel{\bar{M}_x^a} \end{Bmatrix} \rightarrow N_{xs} = L_{22}\gamma_{xs} - \bar{N}_{xs}^a \tag{6}$$

Eq. (6) may also be written in the following form, where G^* is an equivalent shear modulus property of the laminate, and q describes the shear flux:

$$\tau = G^*\left[\gamma_{xs(total)} - \gamma^a{}_{xs}\right] \xrightarrow{\tau = q/t} q = G^* t \left[\overbrace{\frac{\partial u}{\partial s} + \frac{\partial v_t}{\partial x}}^{\gamma_{xs(total)}} - \gamma^a{}_{xs} \right] \tag{7}$$

The tangential displacement is described by the following representation:

$$v_t = r_n\theta \rightarrow \frac{\partial v_t}{dx} = r_n \frac{d\theta}{dx} \tag{8}$$

Substituting Eq.(8) into Eq. (7) yields

$$q = G^* t\left(\frac{\partial u}{\partial s} + r_n \frac{d\theta}{dx} - \gamma^a \right) \tag{9}$$

Integrating the shear flux around the cross section gives

$$\oint_s \frac{q}{G^* t} ds = \oint_s \frac{\partial u}{\partial s} ds + \frac{d\theta}{dx} \oint_s r_n ds - \oint_s \gamma^a ds \tag{10}$$

Eq. (10) could by arranged to show the linking between: cross section geometry, laminate properties, external twist torque, piezoelectric induced strain,

$$\frac{d\theta}{dx} = \frac{T}{4A^2} \oint_s \frac{1}{G^*(s)t(s)} ds - \frac{1}{2A} \oint_s \gamma_{sx}^a(s) ds \tag{11}$$

Integrating Eq.(11) along the airfoil span will give the tip twist angle.

3-2. Finite Elements Model

The closed form solution covers the shear actuation method. To cover all actuation methods and to deal with a more complex design, a finite elements model was built using the ANSYS Multiphysics software , using its Shell99 structural shell layered elements. The structural shell elements do not include piezoelectric properties, therefore the static displacements model was based on the analogy to thermal displacements, namely the piezoelectric coupling coefficient was replaced by the thermal expansion coefficient and the electrical field with the temperature . The model did not include the internal structure of the MFC but the equivalent mechanical and electrical properties supplied by the manufacturer [4] , therefore the actual properties used in the model were free strain per volt and electrical voltage (volts).

$$\alpha \cdot \Delta T \Leftrightarrow d \cdot E \tag{12}$$

4. PARAMETRIC PERFORMANCE INVESTIGATION

One of the major design goals is to reach the optimal design point in a multi parameter environment by using the computational methods mentioned above. To achieve this goal a parametric design performance investigation was performed.

The following Tables describe the materials and laminate properties:

Table 1: Materials mechanical and piezoelectric properties

Property	*MFC*	*E-Glass*
E_1 [GPa]	31.2	14.8
E_2 [GPa]	17.05	13.6
G_{12} [GPa]	5.12	1.9
$_{12}\nu$	0.303	0.19
d_{11} [10^{-12}m/v]	386.63	-
d_{12} [10^{-12}m/v]	-175.5	-
[kg/m^3]ρ	5115.9	1800
Thickness [m]	$3\cdot10^{-4}$	$2.032\cdot10^{-4}$

Table 2: Laminate configuration

Layer #	*Material*	*Orientation*	*Thickness [mm]*	
1	MFC	+45˚	0.3	*
2	E-Glass	0˚	0.2	
3	E-Glass	0˚	0.2	
4	MFC	-45˚	0.3	*

* only in active areas

Table 3 : Laminate equivalent properties

	E_x	E_y	G_{xy}	v_{xy}
Passive areas	15.58 [GPa]	15.04 [GPa]	5.96 [GPa]	0.34
Active areas	14.8 [GPa]	13.6 [GPa]	1.9 9 [GPa]	0.19

The general dimensions of the smart fin are given in Figure , the MFC active area being 58x75 mm^2, the basic airfoil configuration includes two actuators along the span at the top and bottom skin (8 actuators in total), the active area is 24.5% of the wing area, and the tip twist angle is linear with the active skin area.

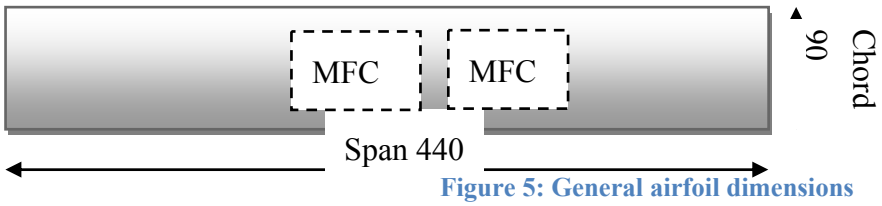

Figure 5: General airfoil dimensions

The twist angle of the airfoils under 500[V] vs. the chord thickness is presented in
Figure , the blue curve calculated by the closed form solution and the green curve is the FEM results.

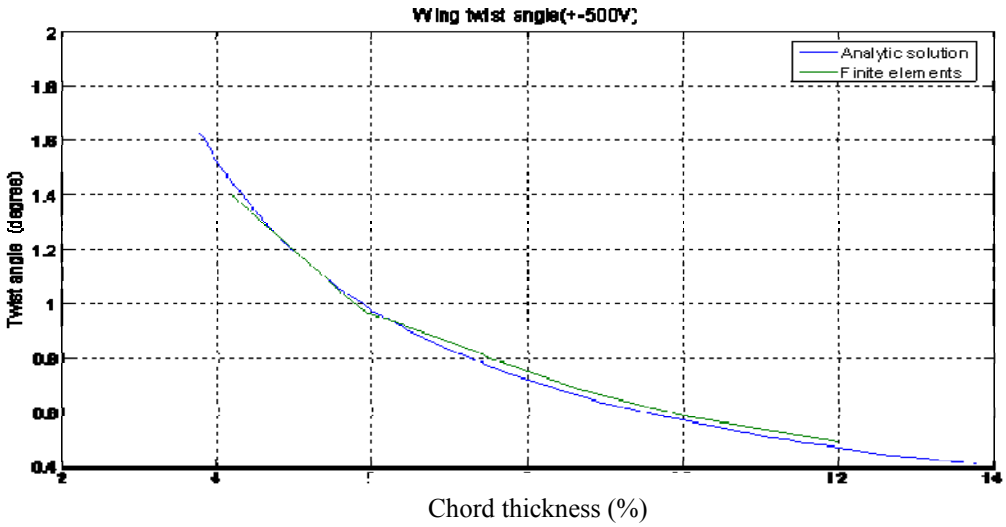

Figure 6: Fin tip twist angle at 500V, with 8 MFC patches, finite elements solution compared with analytic solution, shear actuation method.

Adding aerodynamic load creates strains opposite to the strains induced by the actuators. For a designated aerodynamic limit load an optimal section dimensions exist, that will result in maximum twist angle. Figure displays an example for an aerofoil compliance curve under different aerodynamic loads.

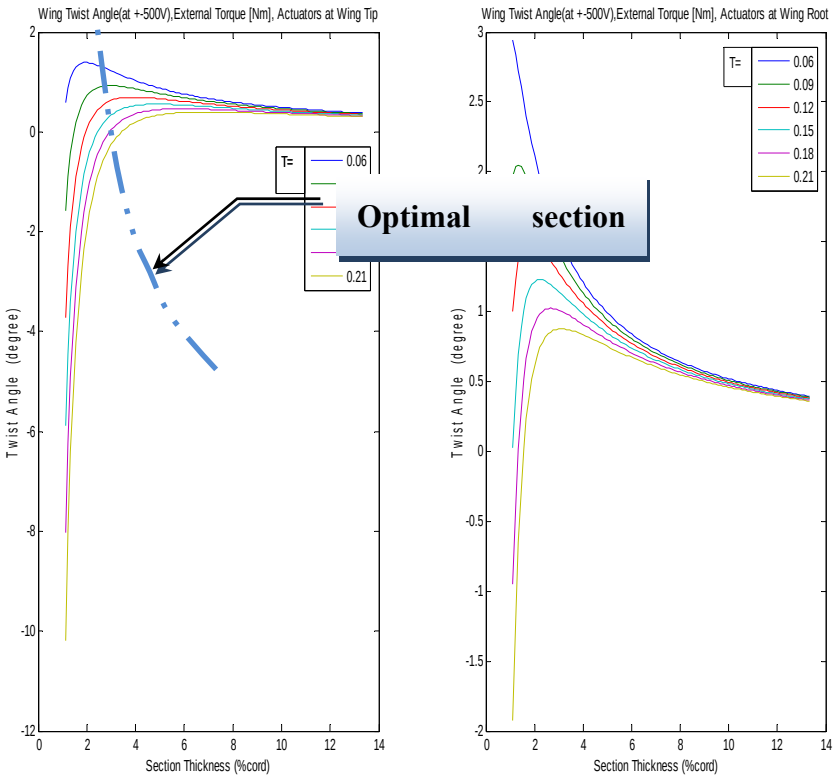

Figure 7 : Twist angle vs. chord thickness under various aerodynamic loads

Combining the optimal chord thickness for each load yields the optimal design curve of the airfoil thickness vs. external loads, an typical example being shown in Figure .

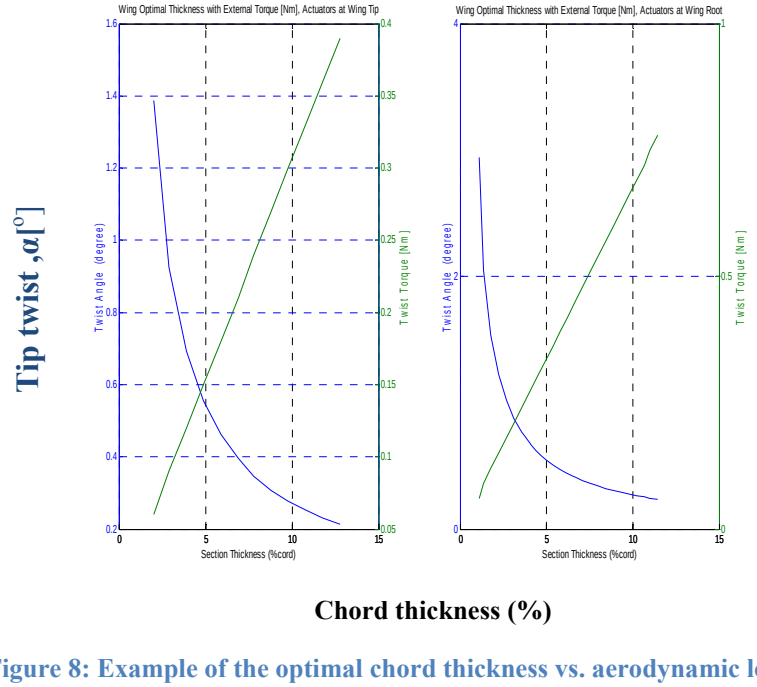

Figure 8: Example of the optimal chord thickness vs. aerodynamic loads

Three basic actuation methods were presented in section 2-2. A comparison between the different methods is shown in Figure . For a single active layer we used only half the number of actuators (green curve), spreading those actuators along the span will give the purple curve, which yields the maximum tip twist. The maximum twist rate per span length is achieved with shear actuation. The skew bending method is the less effective .

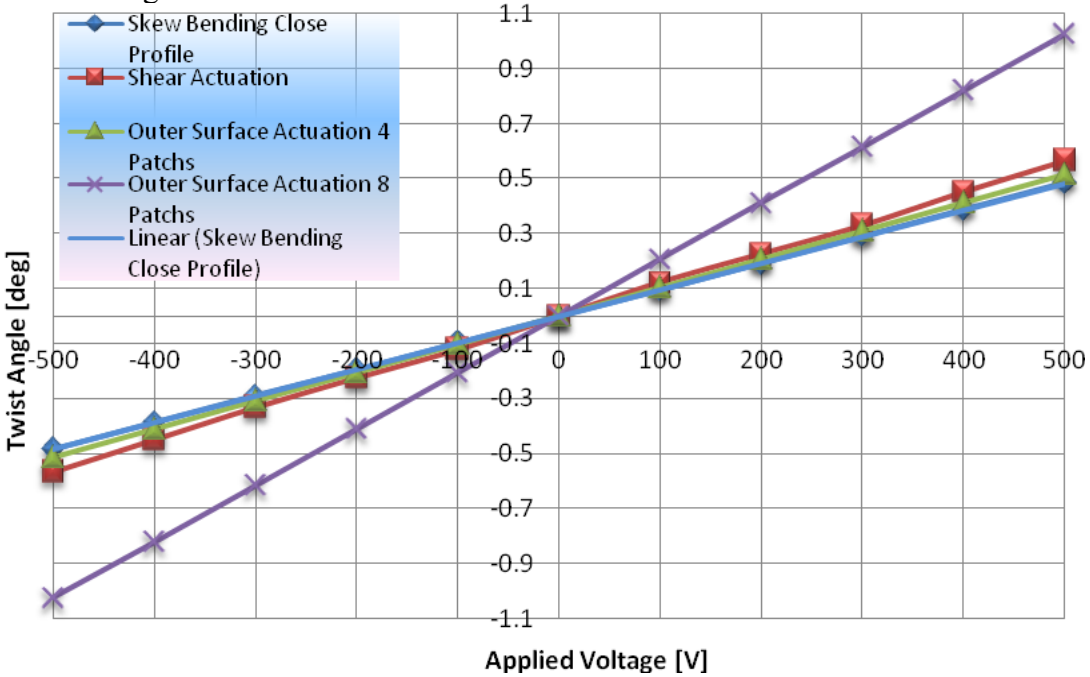

Figure 9: Fin tip twist angle vs. applied voltage for various actuation method, calculated by FEM

The shear method shows optimal results for closed sections and requires continues shear flux, but to get more twist rate an opened or reduced stiffness trailing edge may be used combined with skew bending actuation(see Figure 10). This case shows an improvement of 250% in the tip twist, see Figure 3 .

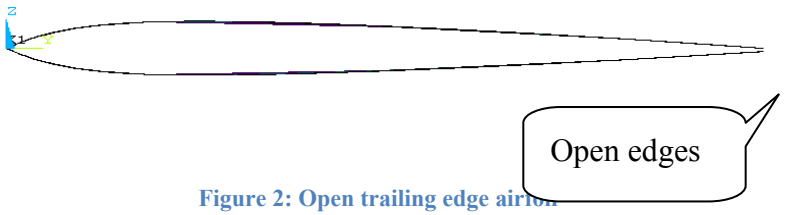

Figure 2: Open trailing edge airfoil

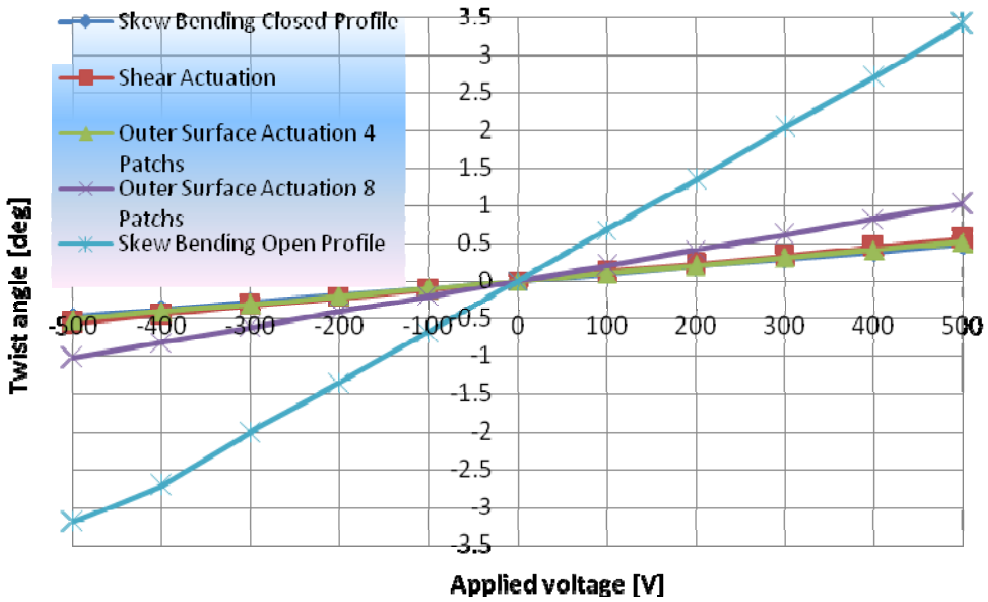

Figure 3: Fin tip twist angle vs. applied voltage for various actuation method including opened trailing edge, calculated by FEM

5. WING DEMONSTRATOR , DESIGN AND MANUFACTURING

The smart wing demonstrator goals are to demonstrate the design concept, verify the computational models and compare between the actuation methods. The skin made of two glass-epoxy layers, and the manufacturing process included production of the bottom and top skins separately in wet lay-up. Next the two MFC actuators couples were bonded to the inner and outer surfaces and electrical wires were routed to the airfoil's root. The wing demonstrator included actuators on one panel only (4 MFC patches in total). The active area of the wing demonstrator skin is 12% of the skin area.

6. RESULTS

Figure 4 presents the results of the complete wing demonstrator lab test and comparison with the FEM results and the analytic closed form solution. The calculated results show good matching with the lab test for shear actuation.

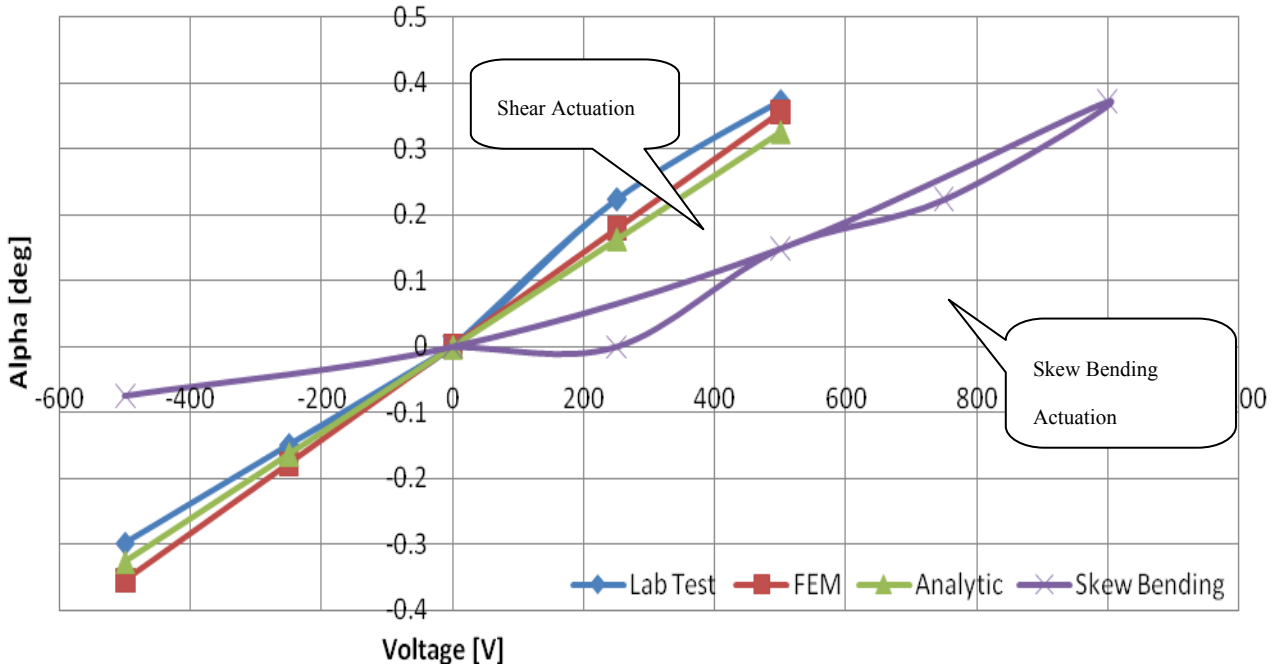

Figure 4: Wing demonstrator lab test results, twist angle vs. electrical power

Because of polarity direction of PZT fibers the electrical field applied on the actuators is non symmetric, the positive direction maximum voltage is 1500 [V] and the negative is -500 [V]. In order to use the maximum field range of the actuators a modified input signal were used, It includes a voltage bias of 250 [V] yielding an improvement in the performance of 150% (see Figure 5). The limitation of 1000 [V] is due to the power supply equipment.

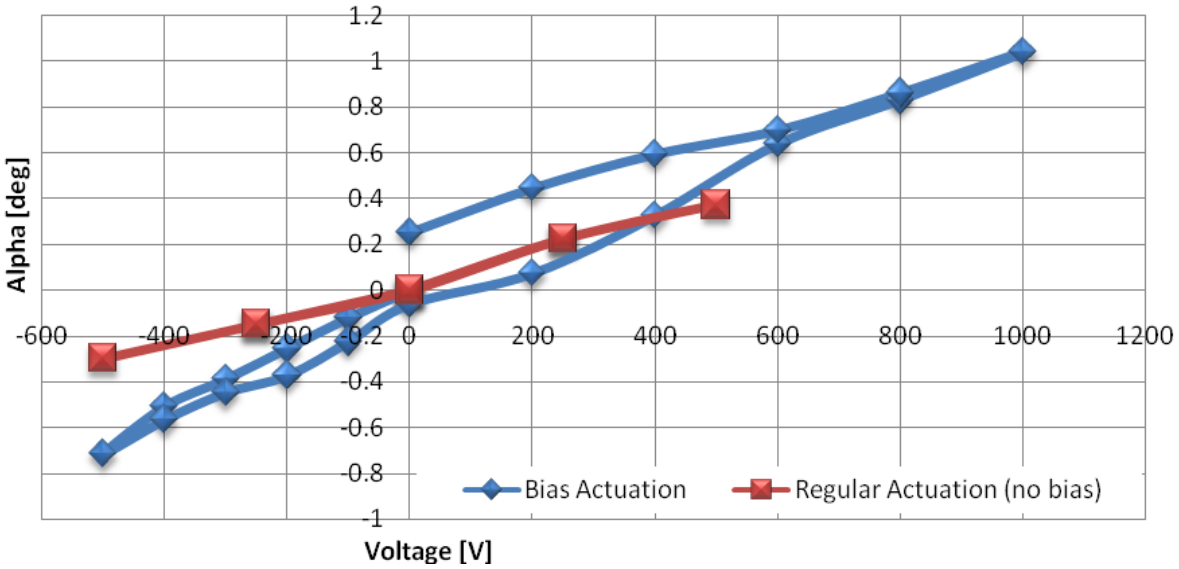

Figure 5: Lab test results, bias actuation

To demonstrate the skew bending with open trailing edge, the two panels forming the wing were attached together using an aluminum foil of 0.3 mm. The foil does not allow a continuous shear flux along the cross section of the airfoil. The results are presented in Figure 6, with the lab results matching the trend of the FEM results.

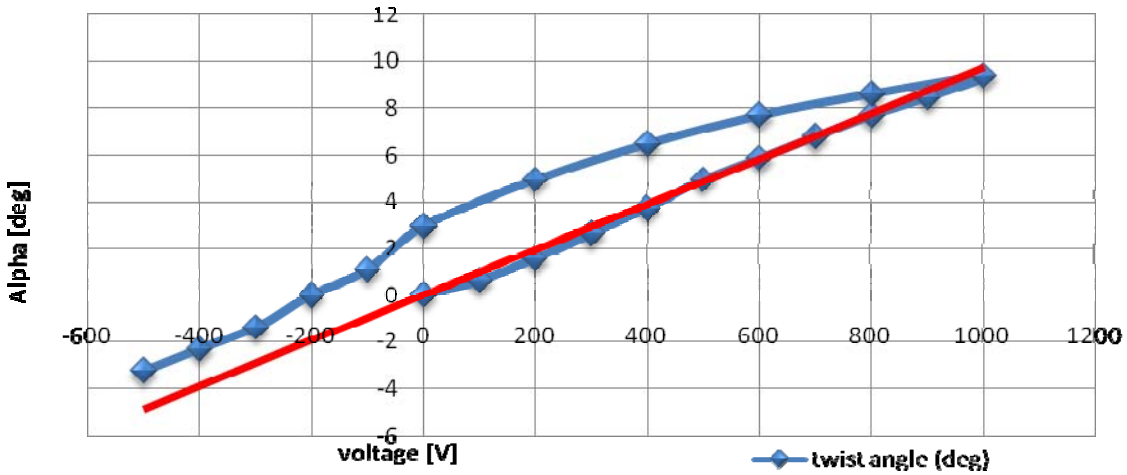

Figure 6: Lab test, skew bending actuation (aluminum foil attached the two panels of the airfoil)

7. CONCLUSIONS

In this study a design concept of a smart piezoelectric control fin with active skin was demonstrated and three actuation methods were suggested, compared and tested. The displacements were calculated by a closed form analytical model and a FEM formulation using shell elements based on the piezoelectric analogy to thermal strains.

A parametric performance investigation was conducted and presented a way for optimizing the geometry of the airfoil cross section. The results of the lab tests showed a good match with the calculated values.

In order to obtain a high performance smart fin, each skin area should be laminated according to its location and role, the active area should be flexible in the actuated directions, and the actuator itself being a part of the structural design, the passive areas should be designed for high stiffness in all directions.

Applying various actuation methods yielded the following:

- The single active layer showed the least effectiveness.
- The shear actuation achieves the greatest twist rate intensity.
- Skew bending actuation improves the airfoil performance if using an opened section; a rigidity decrease is expected in this case and should be taken into consideration.

The smart fin actuator concept may be used for next generation micro UAV's or missiles and answers the need of high aerodynamic efficiency, low weight and minimum volume.

REFERENCES

1. Wilkie, W. K., Bryant, R. G., High, J. W., Fox, R. L., Hellbaum, R. F., Jalink A., lib. D., and Mirick P. H., 2000, ”Low-Cost Piezocomposite Actuator for Structural Control Applications”, Proceeding of the 7th SPIE International Symposium on smart Structures and Materials, Newport Beach, CA, March 5-9.
2. duPlessis A J and Hagood N W 1996, ” Modeling and experimental testing of twist actuated single cell composite beams for helicopter rotor blade control”, MS Dissertation, Department of Aeronautics and Astronautics, Massachusetts Institute of Technology.
3. Matlab , www.mathworks.com
4. Smart Material Corporation .www.smart-materials.com
5. Jae-Sang Park and SangJoon Shin,” A Preliminary Design on the Second Generation Integral Twist-Actuated Blade”, International Conference on Computational and Experimental

Engineering and Sciences, 2007.
6. NASA, National Aeronautic and Space Administration. web site: www.nasa.gov/
7. Robert W. Moses ,Carol D. Wieseman ,Aaron A.Bent, and Alessandro E. Pizzochero, “Evaluation of New Actuators in a Buffet Loads Environment”, NASA Langley Research Center, Continuum Control Corporation.
8. Wilkie, W. K., Bryant, R. G., High, J. W., Fox, R. L., Hellbaum, R. F., Jalink A., Lib, D., and Mirick P. H., 2000, ”Low-Cost Piezocomposite Actuator for Structural Control Applications”, Proceeding of the 7th SPIE International Symposium on smart Structures and Materials, Newport Beach, CA, March 5-9.
9. Wilkie, W. K., Bryant, G. R., High, J. W., “Low-Cost Piezocomposite Actuator for Structural Control Applications,” SPIE 7th Annual International Symposium on Smart Structures and Materials, Newport Beach, CA, 2000.
10. High, J. W. and Wilkie, W. K., “Method of Fabricating NASA-Standard Macro-Fiber Composite Piezoelectric Actuators,” NASA/TM-2003-212427, ARL-TR-2833.